# Steady-State Electron Drift Velocity at Different Temperatures in $Al_XGa_{1-X}N$ and $In_XGa_{1-X}N$ Alloys: Monte Carlo Simulation

**Hamdoune, A., and Bachir, N.**

Unity of Research Materials and Renewable Energies. Faculty of Science. University of Abou-bekr BELKAID. P.O. Box 230. 13000, Tlemcen, Algeria

ahamdoune@gmail.com

**Abstract:** The $Al_xGa_{1-x}N$ and $In_xGa_{1-x}N$ alloys are widely used in optoelectronic devices operating in the visible and ultraviolet. They are also attractive for high power, high temperature and high frequency electronic applications. The specific properties of these materials are the source of the charges induced by the effects of spontaneous and piezo-electric polarizations at the interfaces of quantum wells and super lattices. They are used in heterojunction field effect transistors HFET, modulated doping field effect transistors MODFET, and heterojunction bipolar transistors HBT.
We study $Al_xGa_{1-x}N$ and $In_xGa_{1-x}N$ in the cubic phases because they would have better electronic and optical performances than in their hexagonal phases. We first present GaN, AlN, InN and their alloys $Al_xGa_{1-x}N$ and $In_xGa_{1-x}N$. In the second section; we describe the main steps of Monte Carlo simulation method that we use. In the third section; we calculate steady-state electron drift velocity versus electric field for different temperatures and various molar fractions x. We consider the acoustic, piezo-electric, ionized impurities and polar optical phonon scatterings. We compare our results with published work and are in satisfactory agreement.

**Key words:** AlxGa1-xN, InxGa1-xN, Temperature (T), electric field (E), velocity (v)

## Introduction

The gallium nitride GaN is the most studied of III-N and even more all other semiconductors. Its large gap and its possibility of alloys with indium nitride (InN) and aluminium nitride (AlN) raised great hopes for these materials as devices in both optical and electronic applications (G. Roosen, 2003). The $In_xGa_{1-x}N$ and $Al_xGa_{1-x}N$ alloys are often used as barriers of confinement in the optoelectronic-based nitrides structures, and in transistors such MODFET, HEMT and HBT. Their lattice parameters can be deduced from those of GaN, InN and AlN by Vegard's law; they are given respectively by equations (1) and (2) whose are linear interpolations but not sufficient to obtain more accurate values (Fabrice Enjalbert, 2004). The usual lattice parameters of binary compounds in their cubic phase are given in Table 1. The difference between experimental and theoretical values is due to differences in the quality and structural constraints existing in the layers.

$$a_{In_xGa_{1-x}N} = x \times a_{InN} + (1-x) \times a_{GaN} \qquad (1)$$

$$a_{Al_xGa_{1-x}N} = x \times a_{AlN} + (1-x) \times a_{GaN} \qquad (2)$$

**Table.1** lattice parameters of GaN, InN and AlN compounds, in their cubic phase

| Material | Calculated $a_0$ (Å) (S. K. Pugh et al. 1999) | Experimental $a_0$ (Å) |
|---|---|---|
| GaN | 4.423 - 4.462 - 4.452 | 4.50 (Xu et al. 2000) - 4.53 (R. C. Powell et al. 1993) |
| InN | 4.996 - 4.392 - 4.981 | 4.98 (M. Guerrero and Esteban, 2002) - 4.97 (F. Dessenne, 1998) |
| AlN | 4.301 - 4.392 - 4.34 | 4.38 (I. Petrov et al. 1992) - 4.3996 (Okumaru et al. 1998) |

The effective masses of $In_xGa_{1-x}N$ and $Al_xGa_{1-x}N$ ternary compounds are also often deduced by linear interpolation from those of GaN, InN and AlN. In the Γ valley, they are respectively $m_e^*=0.15m_0$, $m_e^*=0.10m_0$ and $m_e^*=0.25m_0$ in the cubic phase ($m_0$ is the electron mass in vacuum).
At 300K; GaN, InN and AlN admit gaps about 3.2eV, 1.9eV and 6eV in their cubic phases. The variations of the alloys energy band gaps, depending on the composition, are given by equations (3) and (4) where the bowing parameter b is approximately equal to $1.13 \pm 0.23$eV (Fabrice Enjalbert, 2004).

$$E^g_{In_xGa_{1-x}N} = x \times E^g_{InN} + (1-x) \times E^g_{GaN} - b \times x \times (1-x) \qquad (3)$$

$$E^g_{Al_xGa_{1-x}N} = x \times E^g_{AlN} + (1-x) \times E^g_{GaN} - b \times x \times (1-x) \qquad (4)$$

## Monte Carlo Simulation

The Monte Carlo method is based on a drawing of lots process of interactions sustained by the carriers during their movement in the compound, from probability laws. The method consists to follow the behavior of each electron in real space and in wave-vectors space. Let us consider an electron which has energy ε(t), wave-vector k(t), and which is placed in r(t). Under action of an electric field E(r, t); the exchange of energy and momentum with the lattice, and the deviation of its trajectory by impurities, will modify energy, wave-vector and position of the electron. Using mechanical and electrodynamic laws, we determine the behavior of each electron in time and space. To be more realistic:
1. We statistically study possible energy exchange between electrons, modes of lattice vibrations and impurities; this allows us to calculate the probability of these interactions and their effect on the electron energy and wave-vector.
2. We assume that these interactions are instantaneous. We can now do move electrons in free-flight under the only effect of electric field, between two shocks. The free-flight time is determined by drawing lots. When there is interaction, we determine its nature by drawing of lots, and we change the energy and wave-vector of the electron, in this case. The distribution of electrons changes, we then compute the resulting electric field at sufficiently small time intervals. Thus, we can assume the electric field constant between two calculations (Thobel, 1980) – (S. Galden, 1992) – (O. Mouton et al. 1993).

## Results and Discussion

We consider a simplified model of three isotropic and nonparabolic valleys, with a maximum alloy scattering rate. We consider the acoustic, piezoelectric, ionized impurities and polar optical phonon scatterings. We calculate the electron mass in the higher valleys, by the relationship (5) (A.F.M. Anwar et al. 2001) (where m* is their effective mass in Γ valley, and α is the nonparabolicity factor of the considered valley):

$$m = m^* \times (1 + \alpha\varepsilon) \tag{5}$$

In the steady-state, we calculate the electron drift velocity as a function of applied electric field for different temperatures namely 300, 500 and 700K; and for various molar fractions x, in the $Al_xGa_{1-x}N$ and $In_xGa_{1-x}N$ ternary compounds with an electron concentration equal to $10^{17}cm^{-3}$. The results are illustrated respectively by Fig.1 to 6. To validate our results, we compare them with those of reference 14 where the authors study the same ternary compounds, at room temperature.
By increasing the temperature, the gap decreases. That of InN is small; the $In_xGa_{1-x}N$ ternary compound will have its gap towards zero quickly enough. For this reason, we limit ourselves to a temperature equal to 700K.
• Increasing the molar fraction x of aluminium in the $Al_xGa_{1-x}N$ ternary compound, or decreasing the molar fraction x of indium in the $In_xGa_{1-x}N$ ternary compound:
- The band gap energy increases.
- The energy separating the upper valleys and the Γ valley increases; then there is an increasing critical electric field for which the velocity reaches its maximum while the peak velocity decreases.
- The electron effective mass increases also, resulting in a decrease of electron drift velocity.
• At room temperature, we obtain respectively for GaN, InN and AlN peaks about: $3 \times 10^7$cm/s for E=110kV/cm, $3.24 \times 10^7$cm/s for E=50kV/cm and $2.13 \times 10^7$cm/s for E=400kV/cm. Their saturation velocities are respectively about $2 \times 10^7$cm/s, $2.35 \times 10^7$cm/s and $1.75 \times 10^7$cm/s.
• The increase in temperature allows a higher kinetic energy gain for electrons; they move more and then come into collisions with other atoms by transferring their energy. Then for the same molar fraction x; the peak velocity decreases and moves slightly toward the highest fields, and the saturation velocity decreases also.
The alloy scattering mechanism dominates in the ternary compounds under the present simulation conditions; the total scattering rate is higher. Thus a higher field is required to the free carriers for reaching the higher valleys, and the peak velocity occurs at a higher field.
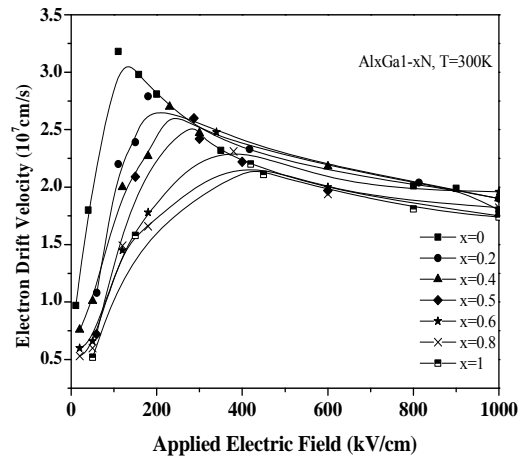
**Fig. 1** The electron drift velocity versus applied electric field for different molar fractions x at 300K, within $Al_xGa_{1-x}N$
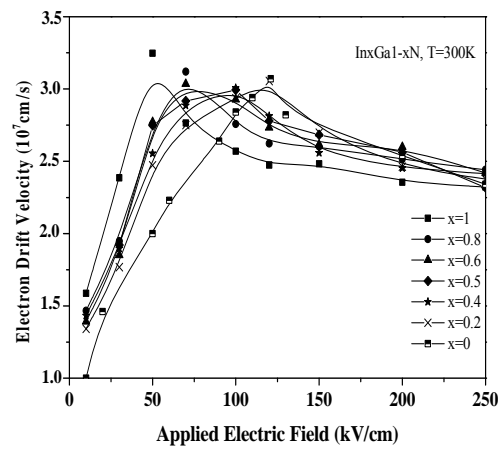


**Fig. 2** The electron drift velocity versus applied electric field for different molar fractions x at 300K, within $In_xGa_{1-x}N$
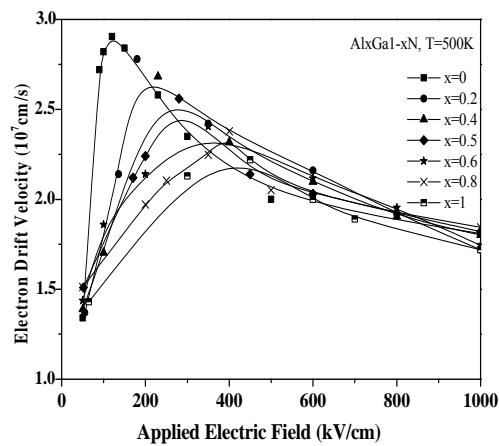


**Fig. 3** The electron drift velocity versus applied electric field for different molar fractions x at 500K, within $Al_xGa_{1-x}N$
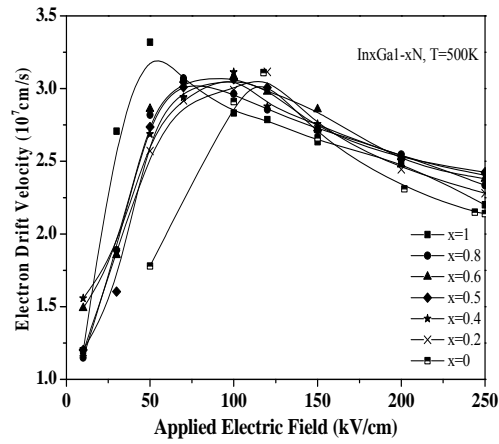
**Fig. 4** The electron drift velocity versus applied electric field for different molar fractions x at 500K, within $In_xGa_{1-x}N$
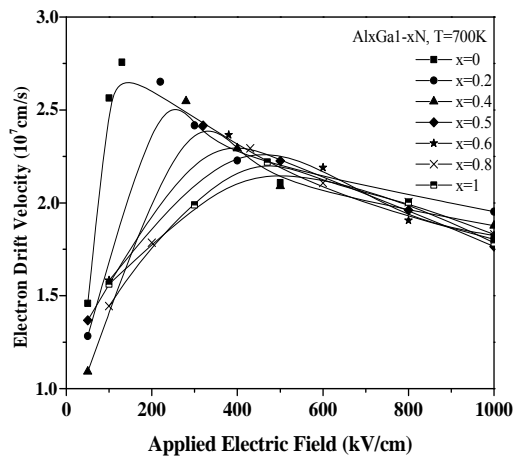


**Fig. 5** The electron drift velocity versus applied electric field for different molar fractions x at 700K, within $Al_xGa_{1-x}N$
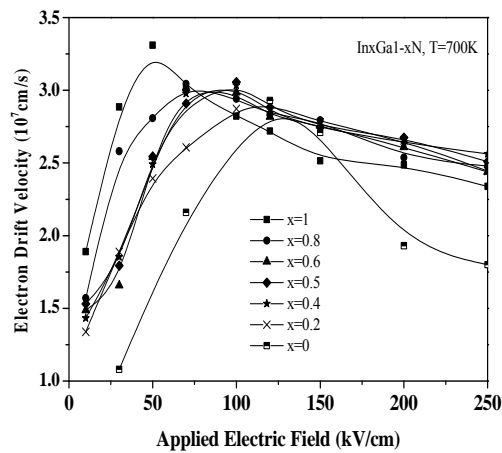


**Fig. 6** The electron drift velocity versus applied electric field for different molar fractions x at 700K, within $In_xGa_{1-x}N$

## Conclusion

GaN, InN, AlN, and their alloys, constitute a major research field of electronics in the solid state for microwave applications. They have several advantages: high voltage thanks to their large gaps, high output impedance, high peak and saturation velocities, and large thermal and chemical stabilities.

We studied the electron transport at low field in the $Al_xGa_{1-x}N$ and $In_xGa_{1-x}N$ ternary compounds, using Monte Carlo simulation, and considering a simplified model of three isotropic and nonparabolic valleys. We considered the acoustic, piezoelectric, ionized impurities and polar optical phonon scattering mechanisms.

We calculated the steady-state electron drift velocity versus applied electric field for different temperatures and various molar fractions x of aluminum and indium in the $Al_xGa_{1-x}N$ and $In_xGa_{1-x}N$ alloys.

The inclusion of alloy scattering influences the transport dynamics changing the peak velocity and the threshold electric field. However, if the alloy scattering is strong, the ternary compounds exhibit peak velocities below that of their constituent binaries.

Calculated at 300K; our results are in satisfactory agreement with those of (M. Farahmand & F. Brennan, 2001) where the authors use a nonparabolic effective mass energy band model, ensemble Monte Carlo simulation.

## References

G. Roosen. (2003). Materials for Optoelectronics, Treaty Series Optoelectronics. Vol. 7, Hermes Science Publications.

Fabrice Enjalbert (2004). Etude des hétérostructures semi-conductrices III-nitrures et application au laser UV pompé par cathode à micropointes. Ph.D. Thesis, University of Joseph Fourier, Grenoble 1, France.

S. K. Pugh, D. J. Dugdale, S. Brand & R.A. Abram (1999). Electronic structure calculation on nitride semiconductors. *Semicond. Technol*, 14, 23-31.

Xu et al. (2000). Anomalous strains in the cubic phase GaN films grown on GaAs (001) by metalogranic chemical vapour deposition. *J. Appl. Phys*. 88(6), 3762-3764.

R. C. Powell, N.E. Lee, Y.W. Kim & J. Greene. (1993). Heteroepetaxial wurtzite and zinc blend structure GaN grown by reactive ion molecular beam epitaxy, growth kinetic microstructure and properties. *J. Appl. Phys.* 73 (1), 189-204.

Martinez Guerrero & Esteban. (2002). Elaboration en épitaxie par jets moléculaires des nitrures d'éléments III en phase cubique. National Institute of Applied Sciences, Lyon, France.

François Dessenne. (1998). Etude thermique et optimisation des transistors à effet de champ de la filière InP et de la filière GaN. Ph.D. Thesis, University of Lille 1, France.

I. Petrov, E. Majob, R.C. Powell & J.E. Greene. (1992). Synthesis of metastable epitaxial zinc blend structure AlN by solid reaction. *J. Appl. phys*, 60(20), 2491-2493.

Okumaru et al. (1998). Growth of cubic III-nitrides by gas source MBE using atomic nitrogen plasma: GaN, AlGaN and AlN. 198, 390-394.

Thobel. (1992). Simulation Monte Carlo du transport électronique et des phénomènes de diffusion dans les systèmes à base de semi-conducteurs III-V. University of Lille 1, France.

S. Galden. (1992). Etude du transistor bipolaire à double hétérojonction Si/SiGe/Si par la simulation Monte Carlo. University of south Paris.

O. Mouton, J. L. Thobel, & R. Fauquemberg. (1993). Monte Carlo simulation of high-field electron transport in GaAs using an analytical band structure model. *J. Appl. Phys*, 10-74.

A.F.M. Anwar, Senior Member, Shangli Wu, & Richard T. (2001). Temperature dependent transport properties in GaN, AlxGa1-xN, and InxGa1-xN semiconductors. *IEEE Transactions on Electron Devices*, 48(3), 567-572.

M. Farahmand & F. Brennan. (2001). Monte Carlo Simulation of Electron Transport in the III-Nitride Wurtzite Phase Materials System: Binaries and Ternaries. *IEEE Trans. Electron Devices*, 48(3).